Pressure-induced melting of charge-order in the self-doped Mott insulator $YNiO_3$

J. L. García-Muñoz
Institut de Ciència de Materials de Barcelona, C.S.I.C., Campus Universitari de Bellaterra, E-08193, Bellaterra, Barcelona, Spain

M. Amboage and M. Hanfland
European Synchrotron Radiation Facility, ESRF, BP 220, F-38043 Grenoble, France

J. A. Alonso and M. J. Martínez-Lope
Instituto de Ciencia de Materiales de Madrid, C.S.I.C., Cantoblanco, E-28049 Madrid, Spain

R. Mortimer
Defence Science Technology Laboratory DSTL, Fort Halstead, Sevenoaks, Kent TN14 7BP, United Kingdom
(Received 4 August 2003; published 10 March 2004)

The stability under pressure of charge order ($Ni^{3+\delta}/Ni^{3-\delta}$) in $YNiO_3$ has been investigated by infrared spectroscopy and x-ray synchrotron diffraction studies up to 23 GPa. We report the observation of a sudden electronic and structural transition in the pressure dependence of $YNiO_3$ at ≈ 14 GPa. The pressure-induced lattice evolution is consistent with a $P2_1/n$ to $Pbnm$ structural transformation similar to the previously reported thermal melting of the charge-ordered state. Phonon screening indicating rapid electron hopping in the high-pressure phase has been observed from infrared measurements. However, although the conductivity increases due to partial charge delocalization, a metallic phase was not confirmed above the pressure-induced transition.

DOI: 10.1103/PhysRevB.69.094106 PACS number(s): 71.30.+h, 71.45.Lr, 71.28.+d

I. INTRODUCTION

The perovskites $R_{1-x}A_xMO_3$ (M=Ni, Mn, and Co) have been the subject of intense experimental investigation during the last decade. Symmetry breaking of spin and orbital degrees of freedom is a common feature in correlated perovskites. In particular, the electronic properties of the $RNiO_3$ perovskite family have received huge interest due to strong correlation effects and a thermally induced metal-insulator (MI) transition.[1–3] A sharp insulator-to-metal transition occurs at a temperature that increases while reducing the ionic radii of the lanthanide ion (135, 201, 403, and 480 K for Pr, Nd, Sm, and Eu, respectively).[1–3] Initially, the I-M transition was ascribed to the closure of a charge transfer gap, producing localization, assuming octahedral coordination, of the Ni^{3+} e_g electron (Ni^{III}:$t_{2g}^6 e_g^1$).[2–4] The isotopic substitution of ^{16}O by ^{18}O revealed the importance of the electron-phonon coupling in the metal-insulator transition.[5] In the insulating state, the magnetic structure has no precedent in perovskite oxides.[6–9] Its unexpected propagation vector $\mathbf{k}=(1/2,0,1/2)$ is difficult to understand in the absence of any kind of orbital ordering.[6–11] Although Ni^{3+} is a Jahn-Teller ion, with a single e_g electron and orbital degeneracy, NiO_6 octahedra are very regular in the $RNiO_3$ family.[3,12]

Due to the difficulty in the preparation of the samples, the compounds with heavier rare earths (RE's) have received little interest until recent years.[12–15] The scenario changed after the discovery of charge disproportionation (CD) in $YNiO_3$.[12] Its structure was found to transform around T_{CD} (ca. 582 K) from monoclinic [$P2_1/n$, hosting a charge density wave (CDW)] to orthorhombic ($Pbnm$, without a CDW) (Ref. 12): $Ni^{3+\delta}+Ni^{3-\delta'}\rightarrow 2Ni^{3+}$, $\delta\approx 0.3e^-$ where $|\delta|\approx|\delta'|$. In the semiconducting monoclinic structure, two types of alternating NiO_6 octahedra are present [$Ni1O_6$ and $Ni2O_6$ with, respectively, expanded (Ni1) and contracted (Ni2) Ni-O bonds]: they signal two different Ni charge states. Although the small monoclinic distortion progressively increases as the lanthanide ionic radius decreases, we did not observe a clear or systematic variation in the amplitude of the charge modulation.[14] Although historical indirect evidence has associated this, now known, change of structure in $YNiO_3$ with an insulator-metal transition, to date no direct electrical data are available confirming the temperature dependence of the electrical properties of $YNiO_3$.

The existence of a charge-modulated or charge-ordered state in the insulating phase of the compounds with lighter (from Dy to Pr) lanthanides has, until recently, been a long-standing open question.[13,16] The difficulties for detecting a symmetry breaking at T_{MI} increase extraordinarily for bigger rare earths. Zaghrioui *et al.*,[17] first, and Staub *et al.*,[18] later, using different experimental techniques found evidence in $NdNiO_3$ supporting a common scenario of charge order for all RE ions.

Two studies of the electrical resistance under pressure in $PrNiO_3$ and $NdNiO_3$ were reported by Canfield[19] *et al.* and Obradors *et al.*[20] in 1993 ($P<1.6$ GPa). The first found that T_{MI} decreases with pressure at a rate $\partial T_{MI}/\partial P=-42$ K/GPa, whereas this rate is, for the same compounds, -76 K/GPa according to Ref. 20. The discrepancy is related to the different cooling and heating rates used in both cases.[21] Strong hysteresis in the resistance is found, varying the temperature across the first-order MI transition. Moreover, reentrant metallic and thermal history effects were observed in transport measurements due to incomplete relaxation processes.[19–21] A comparison of the crystal structure of

$PrNiO_3$ at ambient pressure and 0.5 GPa suggested a small increase of the Ni-O-Ni angle and a decrease of the Ni-O distances under pressure.[21] Here, we present a study of the stability under pressure of charge order of $Ni^{3+\delta}$ and $Ni^{3-\delta'}$ in the insulating phase of $YNiO_3$ using infrared spectroscopy and synchrotron diffraction techniques up to 23 GPa. We show that $YNiO_3$ undergoes a pressure-induced transition at ≈ 14 GPa, related to the collapse of the modulated pattern of self-trapped electrons.

II. EXPERIMENTAL DETAILS

$YNiO_3$ was prepared as polycrystalline powder by high-pressure solid-state reaction (at a pressure of 20 kbar and 900 °C), using a piston-cylinder press.[13] Powder was pressed into pellets and sintered again at high oxygen pressure and temperature. Extensive characterization of our material has been reported elsewhere.[12,14,15] Variable-temperature infrared (IR) measurements (15–800 K) were made using a Nicolet Magna 760 spectrometer (400–4000 cm^{-1}, deuterated triglycine sulfate detector) and a custom-built Oxford Instruments cryostat. $YNiO_3$ was suspended in KBr, the temperature of the sample being measured with a Pt resistance thermometer buried in the sample holder. Variable-pressure measurements were made with a Nicolet Protégé 460 spectrometer ($\approx$480–4000 cm^{-1}), using a diamond anvil cell (DAC). A liquid-nitrogen-cooled cadmium mercury telluride (CMT, type B) detector operating near 78 K was used. Diamond anvil culets of 0.5 mm were used along with gaskets with an aperture diameter of about 0.2 mm. $YNiO_3$ was suspended in NaBr containing 0.3 %W $NaNO_2$ acting as internal pressure sensor.[22] In both domains, measurements were made a number of times to confirm reproducibility.

Diffraction data of $YNiO_3$ under pressure were collected at ambient temperature by angle-dispersive ($\lambda = 0.4166$ Å) x-ray powder diffraction at the beamline ID9 of the European Synchrotron Radiation Facility (ESRF) in Grenoble. A diamond anvil cell was used for pressure generation, with nitrogen as the pressure medium. Synchrotron x-ray diffraction (SXRD) patterns were recorded on image plates and then integrated to obtain intensity versus 2Θ data.[23] Pressures were measured by the ruby luminescence method.[24] Diffraction data were analyzed using the program FULLPROF.[25] We collected SXRD patterns up to 23 GPa on $YNiO_3$ from two different sample loadings, yielding fully reproducible results.

III. RESULTS AND DISCUSSION

A. Infrared spectroscopy

Within our variable parameter constraints, at any temperature (ambient pressure, outside the DAC) or any pressure (ambient temperature, inside the DAC), we measured the signal transmitted by the sample in K(Na)Br [$I(w)$] and that [$I_0(w)$] transmitted by a pure K(Na)Br pellet (K for ambient pressure measurements and Na for elevated pressure measurements, respectively). The normalized optical density $O_d(w) = \ln[I_0(w)/I(w)]$ is, to a first approximation, proportional to the optical conductivity of the sample. Representative $O_d(w)$ infrared spectra of the insulating phase of $YNiO_3$, $SmNiO_3$, and $NdNiO_3$ (at 298, 18, and 34 K, respectively) are compared in Fig. 1. Data for Sm and Nd oxides in this figure are from Ref. 23. The main phonon frequencies match very well those previously reported, and the greater spectral complexity than for the larger nickelates is the signal of a more severe monoclinic distortion. The spectrum is dominated by a pair of phonon modes around 618/568 cm^{-1}, a more complex multiplet around 488 cm^{-1}, and a multiplet around 426 cm^{-1}. According to analyses by previous workers,[17,27–29] phonon bands between 200 and $\approx$500 cm^{-1} correspond to octahedral distortions (deformation modes) of the extended Ni-O lattice. The bands from displacements of the RE atoms against the Ni-O framework occur in the low-frequency range ($<$200 cm^{-1}).[27] The phonon bands in the spectral region $\approx$525–650 cm^{-1} are assigned to octahedral stretching modes. In Fig. 1 the stretching bands around 575 cm^{-1} are split into a doublet in Y and Sm samples. In $NdNiO_3$ only an asymmetry in the band profile can be observed. A more detailed analysis of the phonon spectrum of this family can be found in Refs. 17 and 24.

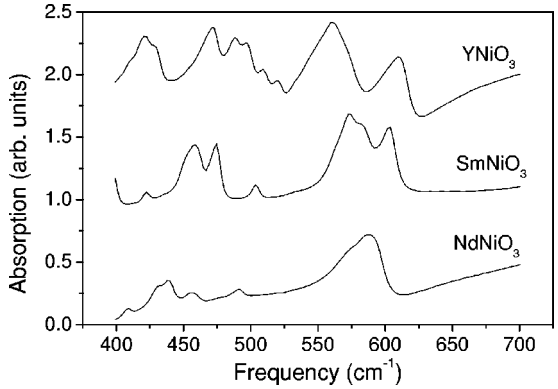

FIG. 1. Infrared spectra (between 400 cm^{-1} and 700 cm^{-1}, ambient pressure) of $YNiO_3$, $SmNiO_3$, and $NdNiO_3$ in the insulating phase (at 298, 18, and 34 K, respectively) (data for Sm and Nd oxides are from Ref. 26).

The temperature dependence of phonon bands in the absorption spectra for $YNiO_3$ and other nickelates was reported in Refs. 24, 27, and 28. As the temperature approaches T_{CD} from the insulating low-temperature phase, band intensities become progressively screened. The loss of spectral intensity does not take place suddenly at T_{CD} but manifests itself in a continuous way up to disappearance near T_{CD} (Ref. 31). In the orthorhombic phase the phonon lines are shielded by a broad background that can be attributed to the mobile electrons. In our sample, the pressure dependence of the infrared spectrum has been measured up to 23 GPa, demonstrating an evolution rather similar to the temperature scan reported by de la Cruz *et al.*[30] The changes induced under pressure in the midinfrared spectra of $YNiO_3$ are shown in Fig. 2, below and above the transition. Our main observation is a pressure-induced transition in $YNiO_3$ around $P_C \approx 14$ GPa. Compared to ambient pressure, phonon band intensities are considerably lower in the elevated pressure range (the intensity is gradually lost), and at $\approx$14 GPa they have practically van-

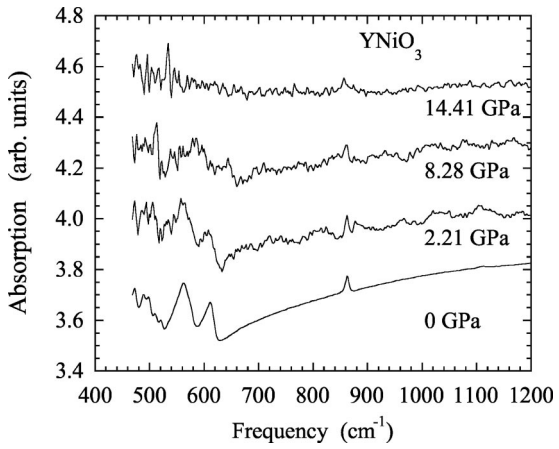

FIG. 2. Pressure dependence of the infrared spectra of YNiO3 between 0 and 17 GPa. Curves have been shifted for the sake of clarity.

ished due to delocalization of the carriers (see data at 14.41 GPa in Fig. 2). We infer that the transition at P_C is accompanied by a significant rise of the electronic conductivity.

The extended base line in Fig. 2 is pressure insensitive towards shorter wavelengths, but shows a strong dependency toward longer wavelengths—in the vicinity of the stretching bands—and is the spectral signature of the optical gap. Thus, in the absorption spectra well below P_C there is a minimum in the background (at $\approx 640\ \mathrm{cm}^{-1}$; see Fig. 2) that gradually decreases increasing the applied pressure. As a measure of changes in the optical gap signature, in Fig. 3(a) we have plotted the pressure dependence of the vertical depth ($\Delta_{\text{max-min}}$), defined as the depth of the minimum referred to the maximum of the adjacent stretching mode ($\approx 625\ \mathrm{cm}^{-1}$). $\Delta_{\text{max-min}}$ shows a relatively strong dependence upon application of an increasing pressure and shows that maximum screening of phonon modes (within our signal-to-noise limitations) is completed at pressures above 13–14 GPa. One can try to extract the optical gap $E_g(P)$ from the wavelength dependence of the optical density of $YNiO_3$. We describe our charge-ordered phase in terms of a traditional semiconductor, using a model of direct band-to-band transitions. Then, the optical edge is such that $[O_d(w) \propto \sigma(\omega)] \propto (\omega - E_g)^{1/2}$ for $\omega > E_g$. Thus, $O_d^2(w)$ versus ω behaves as a straight line above E_g, and a linear extrapolation when $O_d^2(w) \rightarrow 0$ was used to determine E_g. The result is shown in Fig. 3(b). The optical gap begins to diminish upon application of external pressure. However, as shown in this figure, above ≈ 14 GPa the gap becomes almost pressure insensitive within our resolution and, instead of vanishing, it remains constant around 51 meV.

Because of signal-to-noise (S/N) limitations using our DAC, we have repeated the fit using the IR spectrum of $YNiO_3$ measured without the DAC (ca. 15-mm pressed KBr disk). With the much-improved signal/noise ratio, we determined a value for the optical band gap of 70 meV at ambient pressure compared to a band gap extrapolated to zero pressure from DAC data of about 75 meV. Our observation of a nonzero gap above P_C in $YNiO_3$ requires some comments. First, several groups[32,33] have observed differences in photo-

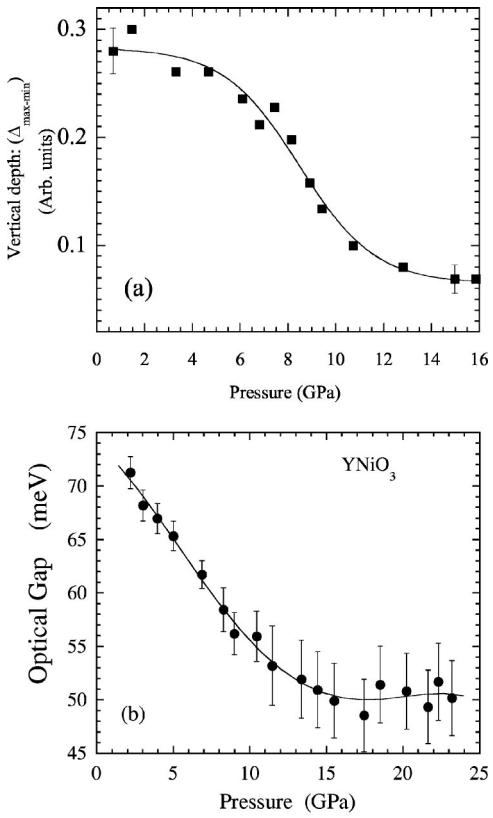

FIG. 3. (a) Pressure dependence of the vertical depth ($\Delta_{\text{max-min}}$), defined as the depth of the minimum referred to the maximum of the adjacent stretching mode at $\approx 625\ \mathrm{cm}^{-1}$. (b) Pressure dependence of the optical gap in $YNiO_3$.

emission experiments between the heaviest (from Dy to Lu) rare earth nickelates and compounds with lighter (from Sm to Pr) lanthanides. From photoemission data a different nature for the metallic phase has been proposed in both cases.[33] One might thus think that the simple semiconductor model of direct band transitions cannot be really applied to all members of this family. Moreover, the material may not be electronically isotropic above P_C, and it could possess anisotropic electrical conductivity. The second aspect is the signal-to-noise limitations using the DAC, which increase substantially at elevated pressures. Overall, these material-intrinsic and material-extrinsic factors make it difficult to determine precise optical gaps. Summarizing, we have observed two different regions under pressure, at both sides of the critical pressure $P_C \approx 14$ GPa. Below P_C the carriers are localized and the optical gap is pressure sensitive. In the second region, above P_C, there is a certain degree of charge delocalization and the optical gap is pressure insensitive. We cannot confirm that the gap has completely closed in $YNiO_3$. Measurements with techniques more suitable for probing the band gap of this material need to be done.

B. Synchrotron x-ray diffraction under pressure

The structural details of these perovskites give valuable information of the changes in the ground state across T_{MI} (Ref. 12). Moreover, it has been demonstrated, at least for

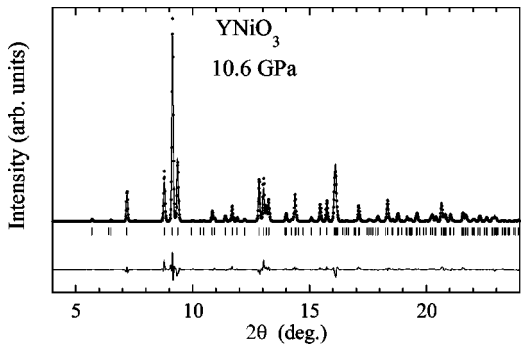

FIG. 4. Rietveld refinement of the SXRD pattern of $YNiO_3$ at 10 GPa (refined using $Pbnm$ symmetry).

the larger RE, that the electron-lattice coupling plays an active role in the temperature induced MI transition of $RNiO_3$.[5] Hence, we studied $YNiO_3$ as well by synchrotron x-ray powder diffraction under pressure at the European Synchrotron Radiation Facility (ESRF, Grenoble). A series of SXRD patterns were collected on ID9 beam line for increasing values of the applied pressure in the range 0–23 GPa. Although the phase presenting charge disproportion has monoclinic $P2_1/n$ symmetry, the deviation from 90° of the monoclinic angle β is actually very small [$\approx 0.07°$ at ambient pressure in $YNiO_3$ (Ref. 12)], too small for being discriminated by the ID9 diffractometer, and thus its detailed evolution under pressure could not be appropriately refined. The diffraction patterns of the sample, in nitrogen as the pressure medium, were not suitable for precise structure refinement using the monoclinic description. Using $Pbnm$ instead of $P2_1/n$ symmetry to describe our patterns of $YNiO_3$ gives no appreciable difference in the goodness of the fit. This is well known to occur in most of $RNiO_3$ oxides from synchrotron x-ray data if the diffractometer is not of ultrahigh resolution. Actually, from our synchrotron x-ray data of $YNiO_3$, it was not possible to distinguish the two octahedral oxygen environments associated with Ni1 and Ni2 sites. The contrast was too weak, precluding us from extracting the evolution with pressure of $Ni1O_6$ and $Ni2O_6$ octahedra in the monoclinic phase. Consequently, Rietveld refinements were made using the conventional $Pbnm$ symmetry, with the atomic positions fixed to the values given in Ref. 15 for the orthorhombic phase (Fig. 4). Full-profile fits including free atomic positions in the orthorhombic description rendered uncertainties too large in the Ni-O distances, which precluded us from monitoring the distortion of the NiO_6 octahedra as a function of pressure. However, the analysis of the lattice evolution reveals interesting features.

The pressure dependence of the lattice parameters is shown in Fig. 5 up to 23 GPa. The lattice evolution under pressure shown in this figure confirms the transition and provides a critical value $P_C \approx 13.5$ GPa (midpoint of the transition). We verified that refinements of the monoclinic cell with the β angle fixed to its ambient pressure value yields the same lattice parameters, within the error, obtained using the average orthorhombic description. Upon increasing pressure, we observe that c discontinuously shrinks at the transition by $\Delta c/c \approx -0.24\%$, while b lengthens by $\Delta b/b \approx 0.10\%$. It

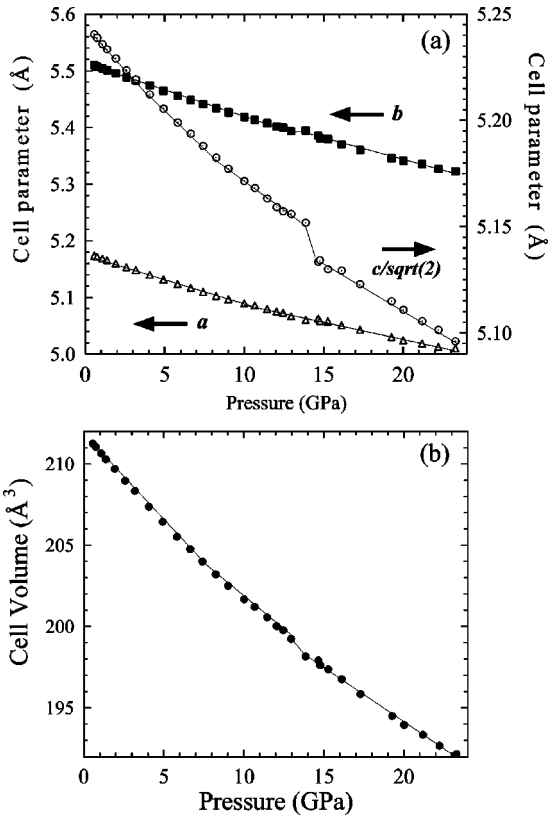

FIG. 5. Pressure dependence of (a) the lattice parameters and (b) the unit cell volume of $YNiO_3$ in the interval 0–23 GPa, across the charge melting transition.

should be emphasized that these changes can be compared, and are qualitatively similar, to those reported at $T_{CD} \approx 582$ K for the thermally induced $P2_1/n \rightarrow Pbnm$ transition: $\approx -0.10\%$ and 0.16%, respectively.[12] A clear change in the evolution of a cannot be appreciated at the transition pressure, as also occurs at T_{CD} (Ref. 12). So the transition is characterized by an anisotropic evolution of the cell comparable to that at T_{CD}. Therefore, the cell evolution under pressure shown in Fig. 5 suggests a structural transition similar to the charge-order melting reported at T_{CD} for the same sample (monoclinic to orthorhombic). Quantitatively we observe some differences. It is worth noticing that the main relative change at the transition in the temperature domain was in the b parameter, whereas under pressure the change in c is much more pronounced than in b. We recall that, upon increasing temperature across T_{CD}, ⟨Ni1-O⟩ bonds contract from 1.994 to 1.958 Å, at the expense of the ⟨Ni2-O⟩ expansion from 1.923 to 1.958 Å. It is of interest to emphasize that the compression of c at the transition pressure is particularly remarkable. As a consequence of this compression the cell volume shrinks by $\Delta V/V \approx -0.10\%$ (plotted in Fig. 5), almost 3 times more than at T_{CD} [$\Delta V/V \approx -0.03\%$ (Ref. 12)].

Further indications of a monoclinic-to-orthorhombic symmetry change across P_C come from a close examination of the profile of the reflections with characteristic monoclinic splitting in the $P2_1/n$ symmetry. Though the weak splitting is not clearly resolved due to its weakness and our limited resolution in the DAC, only these reflections exhibit a certain

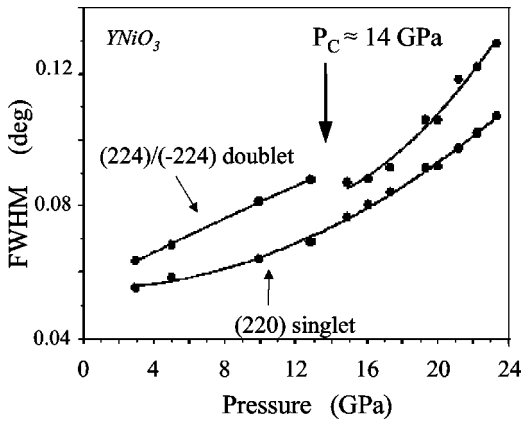

FIG. 6. Variation of FWHM with pressure of $(224)/(-224)$ reflections (doublet in $P2_1/n$ but singlet in $Pbnm$) for $YNiO_3$. The evolution of single reflection (220) (not a doublet for $P2_1/n$ symmetry) is also shown for comparison.

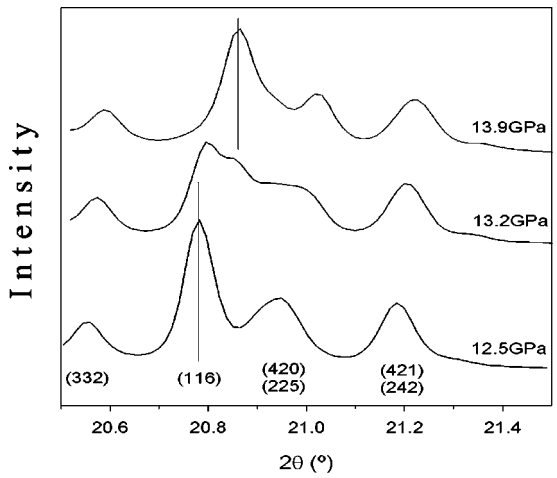

FIG. 7. Selected angular region of the raw SXRD patterns for $YNiO_3$ at three pressures across the transition. The splitting of the (116) peak evidences a two-phase coexistence in a narrow pressure interval around P_C. All the low-pressure phase has transformed above 13.9 GPa.

narrowing above P_C. This is exactly what one expects if the monoclinic doublets collapse at the transition to give an orthorhombic phase. As an example, Fig. 6 shows the pressure dependence of the full width at half maximum (FWHM) of the monoclinic doublet $(224)/(-224)$. A minimum is clearly observed at P_C (Fig. 6) as expected in a sample that becomes orthorhombic. This minimum is never observed in the reflections not split in the monoclinic symmetry. For comparison, the evolution of FWHM for (220) (not a doublet in $P21/n$) is also shown. Moreover, related to the first-order character of the transition, we have observed two-phase coexistence over a narrow pressure interval around 13 GPa. The coexistence of the low- and high-pressure phases is illustrated in Fig. 7. In this figure the peak (116) is observed twice at 13.2 GPa. The peak is observed only once above 14 GPa, signaling that the whole sample has transformed into the high-pressure phase.

IV. CONCLUSIONS

The pressure dependence of the infrared spectrum and x-ray synchrotron diffraction data for $YNiO_3$ were investigated up to 23 GPa. We have observed a pressure-induced melting of charge disproportionation around 14 GPa. This critical pressure separates two different regions: a phase of localized carriers and a phase with at least a degree of charge delocalization. Increasing pressure up to 14 GPa results in a continuous reduction of the optical gap (from 70 meV at ambient pressure to 51 meV in the pressure-independent phase), which suggests a systematic reduction in the amplitude of the charge modulation (2δ) from $2\delta = 0.6e^-/\mathrm{Ni}$ to zero. This is at variance with the temperature evolution of the CO reported in previous investigations (2δ tends sharply to zero, only when T is in the proximity of T_{CD}). In the high-pressure phase, the room-temperature infrared spectra of $YNiO_3$ exhibit the typical phonon screening of a more highly conducting, semiconducting, possibly (partially) metallic system. Our diffraction data confirm that the monoclinic structure and the periodic alternation of $Ni^{3+\delta}$ and $Ni^{3-\delta}$ self-doped species is melted by pressure. Although infrared spectroscopy suggests the melting of charge disproportion ($Ni^{3+\delta} + Ni^{3-\delta} \rightarrow 2Ni^{3+}$) and at least partial delocalization of electron states, the present study cannot confirm the transformation to a metallic state at our highest pressure. However, the anisotropic lattice evolution under pressure is qualitatively similar to the evolution reported across the temperature-driven $P2_1/n \rightarrow Pbnm$ transformation at ambient pressure. Analysis of diffraction data gives a strong indication that the monoclinic symmetry is completely suppressed above 14 GPa. Consequently, diffraction data confirm as well that the periodic alternation of $Ni^{3+\delta}$ and $Ni^{3-\delta}$ self-doped species is melt by pressure.

ACKNOWLEDGMENTS

The authors acknowledge financial support by the Spanish MCyT (Grant Nos. MAT97-0699 and MAT2003-07483-C02-02), Generalitat de Catalunya (Grant No. GRQ95-8029). ESRF is thanked for the provision of x-ray synchrotron diffraction facilities.

[1] P. Lacorre, J. B. Torrance, J. Pannetier, A. I. Nazzal, P. W. Wang, and T. C. Huang, J. Solid State Chem. **91**, 225 (1991).

[2] J. B. Torrance, P. Lacorre, A. I. Nazzal, E. J. Ansaldo, and Ch. Niedermayer, Phys. Rev. B **45**, 8209 (1992).

[3] J. L. Garcia-Munoz, J. Rodriguez-Carvajal, P. Lacorre, and J. B. Torrance, Phys. Rev. B **46**, 4414 (1992).

[4] J. Zaanen, G. A. Sawatzky, and J. W. Allen, Phys. Rev. Lett. **55**, 418 (1985).

[5] M. Medarde, P. Lacorre, K. Conder, F. Fauth, and A. Furrer, Phys. Rev. Lett. **80**, 2397 (1998).

[6] J. L. García-Muñoz, J. Rodríguez-Carvajal, and P. Lacorre, Europhys. Lett. **20**, 241 (1992).
[7] J. L. García-Muñoz, J. Rodríguez-Carvajal, and P. Lacorre, Phys. Rev. B **50**, 978 (1994).
[8] J. L. García-Muñoz, P. Lacorre, and R. Cywinski, Phys. Rev. B **51**, 15 197 (1995).
[9] J. Rodríguez-Carvajal, S. Rosenkranz, M. Medarde, P. Lacorre, M. T. Fernández-Díaz, F. Fauth, and V. Trounov, Phys. Rev. B **57**, 456 (1998).
[10] M. T. Fernández-Díaz, J. A. Alonso, M. J. Martínez-Lope, M. T. Casais, and J. L. García-Muñoz, Phys. Rev. B **64**, 144417 (2001).
[11] J. B. Goodenough, J. Solid State Chem. **127**, 126 (1996).
[12] J. A. Alonso, J. L. García-Muñoz, M. T. Fernández-Díaz, M. A. G. Aranda, M. J. Martínez-Lope, and M. T. Casais, Phys. Rev. Lett. **82**, 3871 (1999).
[13] J. A. Alonso, M. J. Martínez-Lope, M. T. Casais, M. A. G. Aranda, and M. T. Fernández-Díaz, J. Am. Chem. Soc. **121**, 4754 (1999).
[14] J. A. Alonso, M. J. Martínez-Lope, M. T. Casais, J. L. García-Muñoz, and M. T. Fernández-Díaz, Phys. Rev. B **61**, 1756 (2000).
[15] J. A. Alonso, M. J. Martínez-Lope, M. T. Casais, J. L. García-Muñoz, M. A. G. Aranda, and M. T. Fernández-Díaz, Phys. Rev. B **64**, 094102 (2001).
[16] J. A. Alonso, M. J. Martínez-Lope, M. T. Casais, J. L. Martínez, G. Demazeau, A. Largeteau, J. L. García-Muñoz, A. Muñoz, and M. T. Fernández-Díaz, Chem. Mater. **11**, 2463 (1999).
[17] M. Zaghrioui, A. Bulou, P. Lacorre, and P. Laffez, Phys. Rev. B **64**, 081102(R) (2001).
[18] U. Staub, G. I. Meijer, F. Fauth, R. Allenspach, J. G. Bednorz, J. Karpinski, S. M. Kazakov, L. Paolasini, and F. d'Acapito, Phys. Rev. Lett. **88**, 126402 (2002).
[19] P. C. Canfield, J. D. Thompson, S-W. Cheong, and L. W. Rupp, Phys. Rev. B **47**, 12 357 (1993).
[20] X. Obradors, L. M. Paulius, M. B. Maple, J. B. Torrance, A. I. Nazzal, J. Fontcuberta, and X. Granados, Phys. Rev. B **47**, 12 353 (1993).
[21] M. Medarde, J. Mesot, P. Lacorre, S. Rosenkranz, P. Fischer, and K. Gobrecht, Phys. Rev. B **52**, 9248 (1995).
[22] D. D. Klugg and E. Whalley, Rev. Sci. Instrum. **54**, 1205 (1983).
[23] A. Hammersley, computer program FIT2D, ESRF, Grenoble, 1998.
[24] H. K. Mao, J. Xu, and P. M. Bell, J. Geophys. Res. **91**, 4673 (1986).
[25] J. Rodríguez-Carvajal, Physica B **192**, 55 (1993).
[26] R. Mortimer, M. T. Weller, and P. Henry, Physica B **271**, 173 (1999).
[27] M. A. Mroginski, N. E. Massa, H. Salva, J. A. Alonso, and M. J. Martínez-Lope, Phys. Rev. B **60**, 5304 (1999).
[28] T. Crandles, T. Timusk, and J. E. Greedan, Phys. Rev. B **44**, 13 250 (1991).
[29] M. Couzi and P. Van Huong, J. Chem. Phys. **69**, 1339 (1972).
[30] F. P. de la Cruz, C. Piamonteze, N. E. Massa, H. Salva, J. A. Alonso, M. J. Martínez-Lope, and M. T. Casais, Phys. Rev. B **66**, 153104 (2002).
[31] N. E. Massa, J. A. Alonso, M. J. Martínez-Lope, and I. Rasines, Phys. Rev. B **56**, 986 (1997).
[32] I. Vobornik, L. Perfetti, M. Zacchigna, M. Grioni, G. Margaritondo, J. Mesot, M. Medarde, and P. Lacorre, Phys. Rev. B **60**, R8426 (1999).
[33] K. Okazaki, T. Mizokawa, A. Fujimori, E. V. Sampathkumaran, and J. A. Alonso, J. Phys. Chem. Solids **63**, 975 (2002).